https://doi.org/10.5194/angeo-2023-31
Preprint. Discussion started: 4 October 2023

Annales Geophysicae Discussions
Open Access
EGU

Scale Size Estimation of Magnetosheath Jets

Adrian Pöppelwerth[1], Georg Glebe[1], Johannes Z. D. Mieth[1], Florian Koller[2], Tomas Karlsson[3], Zoltan Vörös[4,5], and Ferdinand Plaschke[1]

[1]Institute of Geophysics and Extraterrestrial Physics, Technische Universität Braunschweig, Braunschweig, Germany
[2]Institute of Physics, University of Graz, Graz, Austria
[3]Division of Space and Plasma Physics, School of Electrical Engineering and Computer Science, KTH Royal Institute of Technology, Stockholm, Sweden
[4]Space Research Institute, Austrian Academy of Sciences, Graz, Austria
[5]Institute of Earth Physics and Space Science, HUN-REN, Sopron, Hungary

Correspondence: Adrian Pöppelwerth (a.poeppelwerth@tu-braunschweig.de)

Abstract. Transient enhancements in the dynamic pressure, so-called magnetosheath jets or simply jets, are abundantly found in the magnetosheath. After their formation at the bow shock, they travel through the magnetosheath towards the magnetopause. On their way through the magnetosheath, jets disturb the ambient plasma. In this paper, we use multi-point measurements from the Time History of Events and Macroscale Interactions during Substorms (THEMIS) mission of the motion of ambient magnetosheath plasma responding to the passage of a jet to reconstruct the location of the central axis of that jet, along its propagation direction. This method allows to estimate the spatial distribution of the dynamic pressure within the jet. In addition, the scale size perpendicular to the propagation direction could be estimated for different cross sections. Both dynamic pressure and scale size decrease from the center along the propagation axis towards the rear part.

1 Introduction

The magnetic field of the Earth is an obstacle to the supersonic solar wind. To flow around the magnetopause, the boundary between the terrestrial and interplanetary magnetic fields (IMF), the solar wind must be decelerated to sub-magnetosonic speeds. This takes place upstream at the bow shock where the solar wind is decelerated, heated and deflected.

Depending on the angle θ between the bow shock normal and the IMF, the bow shock can be divided into a quasi-parallel ($\theta < 45°$) or quasi-perpendicular ($\theta > 45°$) shock (e.g., Balogh et al., 2005). Particles reflected at the quasi-parallel shock can travel far upstream along the IMF and interact with the incoming solar wind. This leads to a region called foreshock which hosts a zoo of instabilities and waves (Eastwood et al., 2005). The waves are convected back to the shock with the solar wind, causing a rippled and undulated quasi-parallel bow shock.

The region between the bow shock and magnetopause is called magnetosheath (e.g., Spreiter et al., 1966). In the magnetosheath, localized enhancements in the dynamic pressure are frequently observed. These so-called magnetosheath jets (see the review by Plaschke et al., 2018) were first reported by Němeček et al. (1998). They are observed more often behind the quasi-parallel bow shock (e.g., Vuorinen et al., 2019) which corresponds to low IMF cone angle conditions for the subsolar magnetosheath and favor quiet solar wind (e.g., Plaschke et al., 2013). LaMoury et al. (2021) and Koller et al. (2023) further

https://doi.org/10.5194/angeo-2023-31
Preprint. Discussion started: 4 October 2023

Annales Geophysicae Discussions

investigated the statistical dependence of jet occurrence from solar wind parameters. Jet impact rates determined by LaMoury et al. (2021) showed that more magnetosheath jets impact the magnetopause during low IMF magnitude, low solar wind density and high Mach number conditions. However, the dominant occurrence controlling parameters are low IMF cone angles and high solar wind speeds.

Jet formation downstream of the quasi-parallel bow shock may be explained by a mechanism suggested by Hietala et al. (2009, 2012). At the undulated bow shock, the incoming solar wind will be less decelerated and heated when passing the inclined parts. The geometry of the ripples can cause the flow to converge or diverge, resulting in density increases or decreases behind the shock. This leads to plasma regions with higher velocity and density than in the surrounding magnetosheath. Jets may also form due to solar wind discontinuities interacting with the bow shock (e.g., Archer et al., 2012). For example, Hot Flow Anomalies (HFAs, e.g. Savin et al., 2012) or short large amplitude magnetic structures (SLAMS, e.g. Schwartz and Burgess, 1991) can cause additional shock rippling when passing through the shock (e.g., Karlsson et al., 2018; Raptis et al., 2022). That was also visible in simulations by Suni et al. (2021). They showed that jets can form due to the impact of compressional structures (like SLAMS) at the bow shock, without the detour with the shock ripple approach.

Geoeffective jets (with diameters $> 2R_{\mathrm{E}}$) reach the magnetopause several times per hour (Plaschke et al., 2020a) and have therefore a big impact on the magnetosphere and ionosphere. They can indent the magnetopause (e.g., Shue et al., 2009), cause surface waves (e.g., Archer et al., 2019) and may even penetrate through the boundary (e.g., Dmitriev and Suvorova, 2015). Hietala et al. (2018) showed that jets can trigger and suppress reconnection at the magnetopause. Additionally, upon impact, jets can enhance ionospheric flow channels (Hietala et al., 2012) and disturb radio communication (Dmitriev and Suvorova, 2023). Nykyri et al. (2019) proposed for a single event that jets might even trigger substorms, leading to auroral brightenings. Also, Han et al. (2017) hypothesized in a statistical study that jets impacting the magnetopause are one possible source of throat auroras.

On their way from the bow shock to the magnetopause, plasma jets interact with the ambient magnetosheath plasma. Palmroth et al. (2021) used global hybrid-Vlasov simulations to study the evolution of jets inside the magnetosheath. They reported that the jets thermalize on their way to the magnetopause and become more 'magnetosheath-like' while they keep their propagation direction. Not only the jets but also the ambient plasma is affected from the interaction. Recent studies showed a slight alignment of the magnetic field lines along the jet propagation direction (Plaschke et al., 2020b) and a stirring of the magnetosheath plasma in the vicinity of the jet (Plaschke et al., 2017). Plaschke and Hietala (2018) reported in a statistical analysis of several hundred jets that they push slower plasma ahead of them out of their way. Jets act like plows, and after their passage, the magnetosheath plasma fills the wake regions behind them. They speculated that properties of jets like their scale size may influence the interaction.

Multiple studies report that magnetosheath jets have scale sizes on the order of $1R_{\mathrm{E}}$ in the directions parallel and perpendicular to the jet propagation. To obtain a simple estimation of the parallel size of a jet, it is sufficient to integrate the plasma velocity over the jet observation interval (Plaschke et al., 2020a) or multiply the duration of the jet interval with the maximum speed to get an upper size limit (Gunell et al., 2014). To obtain the perpendicular size at least two spacecraft are needed. Plaschke et al. (2016, 2020a) and Gunell et al. (2014) used pairs of spacecraft and derived the scale sizes in statistical studies

https://doi.org/10.5194/angeo-2023-31
Preprint. Discussion started: 4 October 2023

Annales Geophysicae Discussions
Open Access
EGU

from the probabilities for both spacecraft to observe a jet. Karlsson et al. (2012) used the four Cluster spacecraft (Escoubet et al., 2001) to investigate the scale sizes of single jets. The authors performed a minimum variance analysis to obtain a suitable, jet specific coordinate system. They extrapolated density profiles along these directions with linear fits allowing them to estimate the scale sizes in all 3 directions.

However apart from Karlsson et al. (2012), all aforementioned authors used statistical analyses to obtain information on the scale sizes and other properties of magnetosheath jets. Here we show for the first time the spatial distribution of the dynamic pressure within different cross sections of a jet. Therefore we select a jet event observed by the Time History of Events and Macroscale Interactions during Substorms (THEMIS) spacecraft (Angelopoulos, 2008) to determine the central axis of this jet from the evasive motion of the ambient plasma.

2 Data and Methods

We focus on a jet observed by the THEMIS A, D, and E spacecraft (THA, THD, THE) on 13 October 2010, around 16:04:00 UT. Measurements of the magnetic field (FGM, Auster et al., 2008), ion velocity, ion density, ion energy flux density and dynamic pressure (ESA, McFadden et al., 2008) in the GSE-X direction ($P_{\mathrm{dyn,x}}$) are shown in Fig. 1 (all in spin fit resolution). Following Plaschke et al. (2013), we label the point of maximum dynamic pressure ratio with reference to upstream OMNI measurements (King and Papitashvili, 2005) as t_{max}. Start and end times of the jet interval are labeled as t_{start} and t_{end}, respectively. They denote the times where $P_{\mathrm{dyn,x}}$ equal one quarter of the solar wind dynamic pressure ($P_{\mathrm{dyn,sw}}$). The spacecraft THA, THD and THE observed the jet for 50s, 66s and 43s, respectively.

The rows show from top to bottom, the magnetic field and ion velocity components in GSE coordinates and their magnitudes, the ion density, the ion energy flux density, and the GSE-X component of the dynamic pressure. The ion energy flux density (Fig. 1a4-c4) together with the high ion density (Fig. 1a3-c3) clearly shows that all three spacecraft are in the magnetosheath at the time of the event. The positions in GSE coordinates are given above each column of the figure; they show that all spacecraft are close to the sun-earth line. The dynamic pressure (Fig. 1a5-c5) exhibits for all spacecraft a clear increase above the solar wind value, ensuring that we are indeed observing a jet. The times t_{max} are separated by only 13s and the dynamic pressure peaks resulted from a combined increase in ion density and V_{x} for every spacecraft.

To facilitate the analysis of the measurements, we define a coordinate system that is aligned with the direction of the jet propagation direction and in the rest frame of the ambient magnetosheath plasma. The axes of the new coordinate system are given as follows:

$$\boldsymbol{X'} = \frac{\boldsymbol{V_{\mathrm{Jet}}} - \langle \boldsymbol{V_{\mathrm{MSH}}} \rangle_{15\mathrm{min}}}{|\boldsymbol{V_{\mathrm{Jet}}} - \langle \boldsymbol{V_{\mathrm{MSH}}} \rangle_{15\mathrm{min}}|}, \quad \boldsymbol{Y'} = \frac{\boldsymbol{X'} \times \hat{\boldsymbol{X}}}{|\boldsymbol{X'} \times \hat{\boldsymbol{X}}|}, \quad \boldsymbol{Z'} = \frac{\boldsymbol{X'} \times \boldsymbol{Y'}}{|\boldsymbol{X'} \times \boldsymbol{Y'}|}. \tag{1}$$

For simplicity, we choose $\langle \boldsymbol{V_{\mathrm{MSH}}} \rangle_{15\mathrm{min}}$ to be the mean velocity measured by all three spacecraft in a 15min window around t_{max}. $\boldsymbol{V_{\mathrm{Jet}}}$ is the mean velocity measured by all three spacecraft at their respective t_{max} times and $\hat{\boldsymbol{X}}$ is the unit vector along the GSE-X axis. $\boldsymbol{X'}$ points in the propagation direction of the jet in the ambient plasma rest frame, while $\boldsymbol{Y'}$ and $\boldsymbol{Z'}$ are oriented perpendicular to the propagation direction and complete the right handed system. We shift the time series of velocities and

https://doi.org/10.5194/angeo-2023-31
Preprint. Discussion started: 4 October 2023

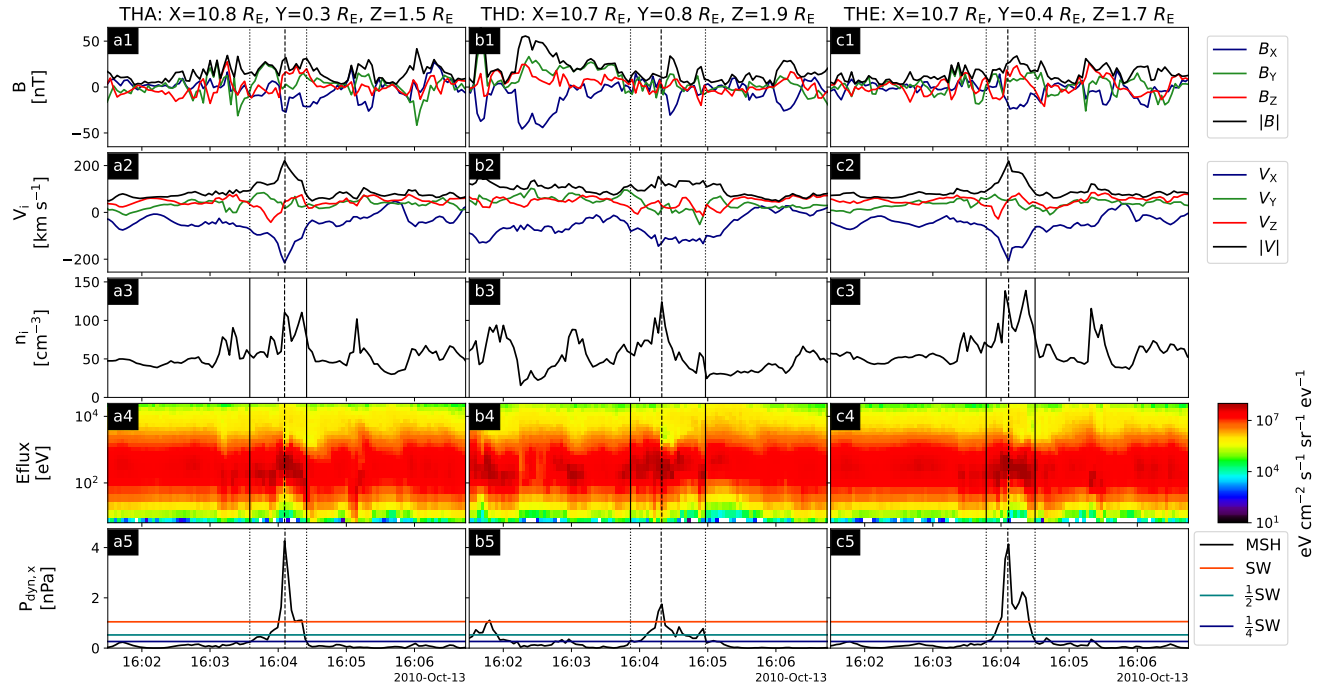

Figure 1. Plasma jet observed by the three THEMIS spacecraft THA (a), THD (b), and THE (c), respectively. From top to bottom, the magnetic field and ion velocity components in GSE coordinates and their magnitudes, the ion density, the ion energy flux density, and the GSE-X component of the dynamic pressure are shown. The vertical dashed lines in each column mark the times of maximum dynamic pressure ratio ($t_{\max}$). The dotted lines denote the start ($t_{\rm start}$) and end times ($t_{\rm end}$) of the jet intervals. The horizontal lines in the last row represent the solar wind dynamic pressure, as well as half and a quarter thereof (in orange, cyan, and blue, respectively).

positions of THA and THE by 13s each so that all spacecraft observe $t_{\max}$ at the same time. We subtract $\langle \boldsymbol{V}_{\mathbf{MSH}} \rangle_{15\mathrm{min}}$ from the measured ion velocities and then transform them into the new coordinate system. The spacecraft positions are transformed directly into the new coordinate system.

The orientations of the ion velocity vectors in the $\boldsymbol{Y'} - \boldsymbol{Z'}$ plane change due to the passage of the jet. This is shown for 9 time steps from 12s before to 12s after $t_{\max}$ in Fig. 2. The arrows indicate the velocities at the spacecraft positions (circles) of THA, THD and THE in red, green and blue, respectively and the black dot represents the estimated center of the jet after Fig. 3. On the left side of the figure, prior to jet passage, the arrows point in different directions. While the velocities at THA and THE point in the positive $\boldsymbol{Y'}$ direction (away from the jet center), at THD the velocity is directed in the opposite direction. Closer to $t_{\max}$ the arrows show a diverging pattern with THA pointing in the positive and THE in the negative $\boldsymbol{Z'}$ direction. The arrow at THD starts to rotate clockwise and points away from the center. Directly in front of $t_{\max}$ the direction of the arrow at THA flips. The overall behavior before the jet passage is therefore rather complicated. In contrast, the arrows on the right side in Fig. 2 corresponding with times after the jet passage point roughly to one point (the jet center) and visualize the converging plasma

https://doi.org/10.5194/angeo-2023-31
Preprint. Discussion started: 4 October 2023

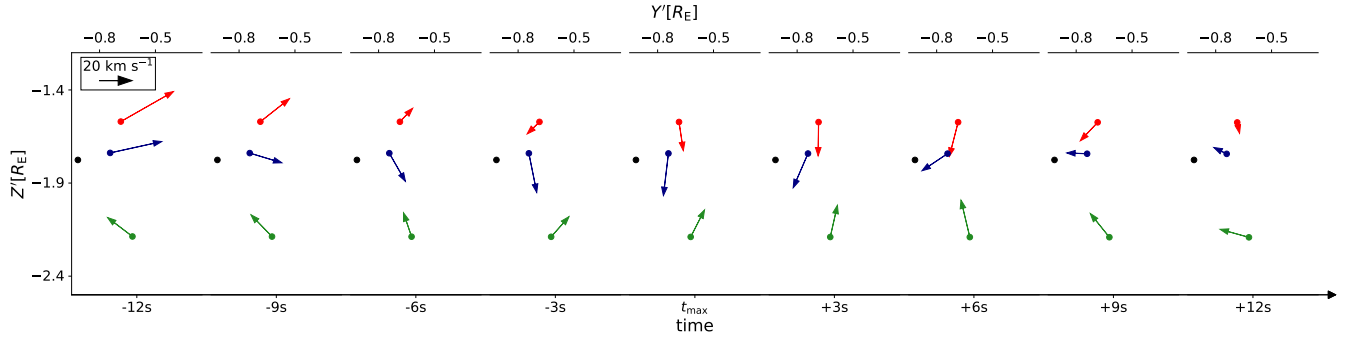

Figure 2. Measured ion velocity, time-averaged over the neighboring data points, at the three spacecraft positions for 9 time steps around $t_{\max}$ in the plane perpendicular to the jet propagation direction in the magnetosheath rest frame. The circles represent the spacecraft positions and the arrows indicate the velocities. The colors for THA, THD, and THE are red, green, and blue, respectively. The black dots at each step represent the estimated center after Fig. 3. The top axis shows the corresponding $\boldsymbol{Y'}$ coordinates for each time step. The $\boldsymbol{Z'}$-axis is the same for each time step. The bottom axis displays the time steps. In the upper left corner, the black arrow indicates the scale.

flows after the jet has passed the spacecraft. These observations can be interpreted as an indication of an evasive motion of the ambient plasma ahead of the jet and the subsequent filling of the wake afterwards, as reported by Plaschke and Hietala (2018).

From the wake-filling plasma flow after the jet passage observed at the three spacecraft positions, we can estimate the position of the jet center. Therefore, we take a closer look at the time 9s after $t_{\max}$ and extend the corresponding velocity vectors in the $\boldsymbol{Y'}$-$\boldsymbol{Z'}$-plane (gray lines in Fig.3). We choose this time step as the converging flow is most clearly seen here. We determine the center as the point whose perpendicular distance to all three lines is minimal. This estimation is shown in Fig.3 with the black dot representing the calculated center. Due to the fact that the $\boldsymbol{Y'}$ and $\boldsymbol{Z'}$ axes are oriented perpendicular to the propagation, the position of the center in this plane should be valid for the entire jet interval, assuming a constant propagation direction.

3 Results

The distances of THA, THD and THE from the center in the $\boldsymbol{Y'}$-$\boldsymbol{Z'}$-plane are $0.31R_{\mathrm{E}}$, $0.51R_{\mathrm{E}}$ and $0.18R_{\mathrm{E}}$, respectively. These values change only marginally (max. 5%) over the jet interval due to the spacecraft movement. We plot $P_{\mathrm{dyn,x}}$ as measured in the spacecraft system against these distances for different times. For $t_{\max}$ this is shown in Fig.4a and for $t_{\max}$+12s it is shown in Fig.4b. Crosses in red, green, and blue represent the data points for THA, THD and THE, respectively. We also plot one quarter of the solar wind dynamic pressure (blue horizontal line) in Fig.4 and fit a Gaussian distribution with an additional offset corresponding to the background dynamic pressure (black dashed line):

$$P_{\mathrm{dyn,fit}} = P_0 \cdot \exp\left(\frac{-r^2}{2 \cdot \Delta R^2}\right) + P_{\mathrm{dyn,BG}}. \tag{2}$$

https://doi.org/10.5194/angeo-2023-31
Preprint. Discussion started: 4 October 2023

Annales Geophysicae Discussions
Open Access
EGU

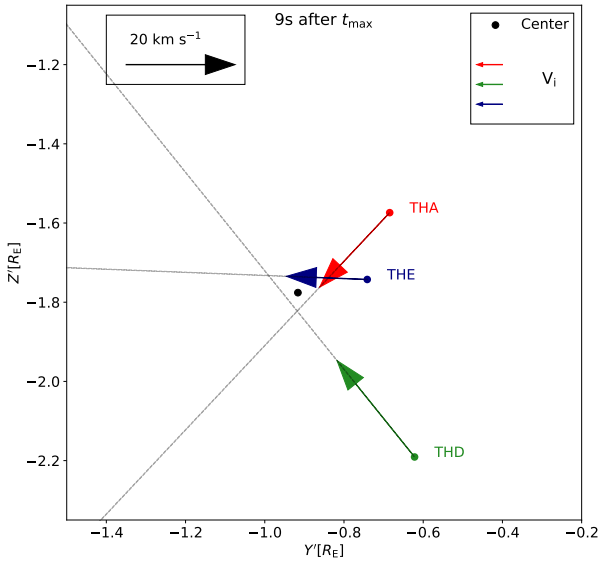

Figure 3. Measured ion velocity, time-averaged over the neighboring data points, at the three spacecraft positions 9s after t_{max} in the plane perpendicular to the jet propagation in the magnetosheath rest frame. The circles represent the positions of the spacecraft and the arrows indicate the velocity. The colors for THA, THD, and THE are red, green, and blue, respectively. The black arrow indicates the scale. The gray lines are simple extensions of the velocity vectors, and the black dot marks the closest point to the three lines and represents the center position. The estimated center is also included in Fig. 2.

Here the fit parameters P_0 and ΔR give the amplitude and width of the Gaussian. $P_{\rm dyn,BG}$ is the background dynamic pressure in GSE-X direction and r the distance to the center. To determine $P_{\rm dyn,BG}$, we average the values for $P_{\rm dyn,x}$ measured by all three spacecraft within a 15min window around $t_{\rm max}$. This results in $P_{\rm dyn,BG}$ =0.05nPa. The intersection of the fit with $P_{\rm dyn,x} = \frac{1}{4}P_{\rm dyn,sw}$ =0.26nPa leads to a estimation of the jet size in the direction perpendicular to the jet propagation. We choose one quarter of the solar wind dynamic pressure as a threshold to be consistent with the definition of $t_{\rm start}$ and $t_{\rm end}$ for jets, which determine the scale size along the jet propagation (see criterion of Plaschke et al., 2013). For this estimation, we assume a radially symmetric profile of the dynamic pressure around the propagation axis.

At both times, the dynamic pressure increases towards the center. While in Fig.4a the value at THA (further away from the center) is slightly higher than at THE, the fit in Fig.4b represents the data points very well. The fit parameters are P_0 =4.98nPa and ΔR =0.38$R_{\rm E}$ for the time $t_{\rm max}$ and P_0 =2.90nPa and ΔR =0.23$R_{\rm E}$ for $t_{\rm max}$+12s. The estimated central jet dynamic pressure is higher at $t_{\rm max}$ (5nPa) than at $t_{\rm max}$+12s (3nPa). Therefore the dynamic pressure decreases along the central jet axis towards the rear part of the jet. The Gaussian fits intersect the horizontal line at 0.96$R_{\rm E}$ and 0.52$R_{\rm E}$ at $t_{\rm max}$ and $t_{\rm max}$+12s, respectively. This corresponds with a larger perpendicular size of the jet around $t_{\rm max}$ and a decrease of the size towards the rear part.

https://doi.org/10.5194/angeo-2023-31
Preprint. Discussion started: 4 October 2023

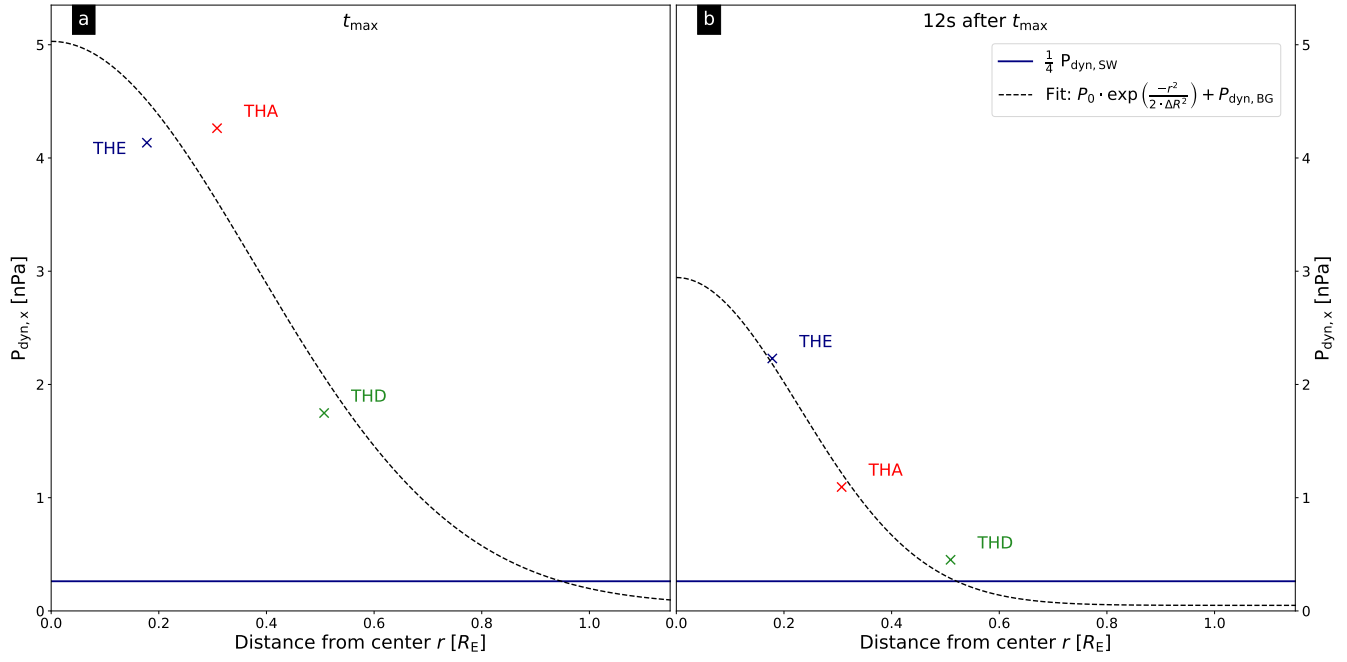

Figure 4. Dynamic pressure $P_{\mathrm{dyn,x}}$ as measured in the spacecraft system versus the distance from the center r at THA, THD and THE (crosses in red, green and blue, respectively) at t_{max} (a) and at 12s after t_{max} (b). The dashed line represent a fit with a Gaussian distribution with an offset corresponding to the dynamic pressure of the background magnetosheath (black). The blue horizontal line depicts a quarter of the solar wind dynamic pressure.

4 Discussion

The ideal scenario of the evasive motion of ambient plasma around a jet as described by Plaschke and Hietala (2018) consists of a clear diverging plasma flow ahead of the jet and a subsequent converging flow behind, as the ambient plasma fills the wake left by the jet. A look at Fig. 2 suggests that signs of the latter are visible; the converging plasma flow can be observed. In contrast, the diverging flow is not clearly visible. Especially for THD the flow deviates from the expectation. Additionally the velocity at THA points towards the center even slightly before t_{max}. This could be the result of a more complex jet with an irregular shape associated with local turbulence generation. Alternatively a second jet may be passing by causing a complex flow pattern. The significant deviation from the average situation described by Plaschke and Hietala (2018) does not allow further interpretation of the flow pattern before t_{max}. Nevertheless, the converging flow after the jet passage is clearly recognizable with all arrows pointing towards the center on the right side of Fig. 2. This flow pattern allows us the determination of the jet center as shown in Fig. 3. The position of the center together with radial distances of the spacecraft lead to the estimation of the scale sizes perpendicular to the propagation direction. To verify the results obtained, we compare the estimated scale sizes with previous results.

https://doi.org/10.5194/angeo-2023-31
Preprint. Discussion started: 4 October 2023


Annales Geophysicae Discussions

In previous studies, different authors reported a range of scale sizes of magnetosheath jets. Plaschke et al. (2020a) derived that most of the jets should be on the order of $0.1R_{\mathrm{E}}$, although they argued that these small jets are less likely to be observed. For the observed magnetosheath jets, they report a median diameter of about $1R_{\mathrm{E}}$ in the directions parallel and perpendicular to the flow. Gunell et al. (2014) calculated upper limits and found median values of $4.9R_{\mathrm{E}}$ and $3.6R_{\mathrm{E}}$ for the sizes parallel and perpendicular to the flow, respectively. Both studies used pairs of spacecraft and the probabilities that both observe a jet to calculate sizes perpendicular to the propagation directions. Karlsson et al. (2012) found scale sizes between 0.1 and $10R_{\mathrm{E}}$ for one direction perpendicular to the magnetic field; for the other two dimensions the sizes were found to be a factor of 3-10 larger. Thus our results with diameters of approximately $2R_{\mathrm{E}}$ at $t_{\max}$ and $1R_{\mathrm{E}}$ at $t_{\max}$+12s fit very well to the earlier reported sizes.

The method presented by Karlsson et al. (2012) can be used to obtain the sizes of single jet events in all three dimensions. This is only possible if the structure is associated with a magnetic field discontinuity, which was the case for all their events. Contrary to this, our method provides scale sizes for the directions parallel and perpendicular to the flow under the assumption of rotational symmetry. Furthermore, we assume a constant propagation direction and radial dynamic pressure profiles that resemble Gaussian distributions. The problem can thus be reduced to two dimensions. This then gives us the possibility to estimate the perpendicular scale size for different cross sections of a jet. Together with the parallel scale size, we could create a simple 3D model of the magnetosheath jet. To apply this method, it is necessary to observe the flow pattern of the ambient magnetosheath plasma reported by Plaschke and Hietala (2018). At least one of the two motions - diverging or converging plasma flow - is required to determine the position of the jet center. Thus, this estimation is not applicable to all jets observed by multiple spacecraft, as individual events can deviate strongly from the average behavior. As Plaschke et al. (2020b) have shown for the alignment of velocity and magnetic field, the fluctuations can easily be on the same order of magnitude as the average alignment effect. Also in this case study, we don't see a clear diverging flow ahead of the jet.

Note that the method described in this paper relies on further assumptions and simplifications. We assume rotational symmetry of the dynamic pressure distribution around the central axis that is aligned with the constant propagation direction. The choice of the Gaussian distribution for the fit implies a corresponding monotonous decrease of the dynamic pressure from the center towards the edges. Both assumptions may not be necessarily satisfied in general or in some parts of the jet. To perform our analysis we need at least three spacecraft. More spacecraft observing the same jet or the ambient magnetosheath would allow an evaluation of the validity of our assumptions.

5 Summary and Conclusion

We observed the flow pattern of the ambient plasma due to the passage of a jet with the three THEMIS spacecraft THA, THD and THE. From the converging plasma flow after jet passage we were able to estimate the position of the jet central axis. The distances of the spacecraft from the central axis together with the measured $P_{\mathrm{dyn,x}}$ was used to fit a Gaussian distribution with an additional offset corresponding to the background dynamic pressure. This was shown for different times ($t_{\max}$ and $t_{\max}$+12s) with the following two results:

https://doi.org/10.5194/angeo-2023-31
Preprint. Discussion started: 4 October 2023

Annales Geophysicae Discussions

1. The dynamic pressure in the central part of the jet is higher at $t_{\max}$ (5nPa) and decreases towards the rear part (3nPa),
2. The perpendicular size of the jet is larger at $t_{\max}$ ($2R_{\mathrm{E}}$) and decreases towards the rear part ($1R_{\mathrm{E}}$).

The larger scale size around $t_{\max}$ suggests that some spacecraft may only observe central parts of a jet rather than the front and rear parts when passing through edge regions. In addition, spacecraft will unlikely observe the exact center of a jet. Thus, they would measure just a fraction of the dynamic pressure in the jet center (a lower limit) as $P_{\mathrm{dyn,x}}$ decreases towards the edges and this would not be representative for the jet. This implies that statistical studies of dynamic pressures of jets significantly and systematically underestimate the maximum values (e.g., Raptis et al., 2020).

Finally, the larger expansion near $t_{\max}$ leads to longer observation times by spacecraft passing the central region of jets. In contrast, the dynamic pressure at the front and rear parts falls below the detection threshold earlier, leading together with the faster decrease of $P_{\mathrm{dyn,x}}$ (corresponds to smaller ΔR) to shorter spacecraft observation times.

The jet event selected for this case study belongs to a small fraction of jet measurements that show signs of the expected flow pattern that is needed for the estimation of the center. With only three spacecraft available, there are uncertainties regarding the quality and applicability of the fit and validity of our assumption of rotational symmetry. To increase our confidence in the fit and our assumptions, it would be useful to obtain measurements from even more spacecraft on a jet. This could be achieved through conjunctions of spacecraft from different missions like Cluster, Magnetospheric Multiscale (MMS, Burch et al., 2016) and THEMIS.

Data availability. Data from the THEMIS mission including level 2 FGM and ESA data are publicly available from the University of California Berkeley and can be obtained from http://themis.ssl.berkeley.edu/data/themis (THEMIS, 2023). The solar wind data from NASA's OMNI high-resolution data set (1 min cadence) are also publicly available and can be obtained from https://spdf.gsfc.nasa.gov/pub/data/omni/omni_cdaweb (OMNI, 2023). THEMIS and OMNI data were accessed using the PySPEDAS software (Grimes et al., 2018; Angelopoulos et al., 2019).

Author contributions. AP performed the main work. GG, FK, TK, ZV and FP helped with the discussions and interpretations of the results. JM took care of THEMIS FGM calibration and brought his expertise on THEMIS data into the discussions.

Competing interests. The authors declare that they have no conflict of interest.

Acknowledgements. We acknowledge NASA contract NAS5-02099 for use of data from the THEMIS Mission, specifically C.W. Carlson and J. P. McFadden for the use of ESA data; K. H. Glassmeier, U. Auster, and W. Baumjohann for the use of FGM data provided under the lead of the Technical University of Braunschweig and with financial support through the German Ministry for Economy and Technology and

https://doi.org/10.5194/angeo-2023-31
Preprint. Discussion started: 4 October 2023

Annales Geophysicae Discussions
Open Access
EGU

the German Center for Aviation and Space (DLR) under contract 50 OC 0302. This work was financially supported by the German Center for Aviation and Space (DLR) under contract 50 OC 2201. FK and ZV acknowledge the support by the Austrian Science Fund (FWF), P 33285-N.

https://doi.org/10.5194/angeo-2023-31
Preprint. Discussion started: 4 October 2023

Annales Geophysicae Discussions
Open Access
EGU

References

Angelopoulos, V.: The THEMIS Mission, Space Sci. Rev., 141, 5–34, https://doi.org/10.1007/s11214-008-9336-1, 2008.

Angelopoulos, V., Cruce, P., Drozdov, A., Grimes, E. W., Hatzigeorgiu, N., King, D. A., et al.: The Space Physics Environment Data Analysis System (SPEDAS), Space Sci. Rev., 215, 9, https://doi.org/10.1007/s11214-018-0576-4, 2019.

Archer, M. O., Horbury, T. S., and Eastwood, J. P.: Magnetosheath pressure pulses: Generation downstream of the bow shock from solar wind discontinuities, J. Geophys. Res.-Space, 117, https://doi.org/https://doi.org/10.1029/2011JA017468, 2012.

Archer, M. O., Hietala, H., Hartinger, M. D., Plaschke, F., and Angelopoulos, V.: Direct observations of a surface eigenmode of the dayside magnetopause, Nat. Commun., 10, https://doi.org/10.1038/s41467-018-08134-5, 2019.

Auster, H., Glassmeier, K., Magnes, W., andW. Baumjohann, O. A., Constantinescu, D., Fischer, D., Fornacon, K., Georgescu, E., Harvey, P., Hillenmaier, O., Kroth, R., Ludlam, M., Narita, Y., Nakamura, R., Okrafka, K., Plaschke, F., Richter, I., Schwarzl, H., Stoll, B., Valavanoglou, A., and Wiedemann, M.: The THEMIS Fluxgate Magnetometer, Space Sci. Rev., 141, 235–264, https://doi.org/10.1007/s11214-008-9365-9, 2008.

Balogh, A., Schwartz, S. J., Bale, S. D., Balikhin, M. A., Burgess, D., Horbury, T. S., Krasnoselskikh, V. V., Kucharek, H., Lembège, B., Lucek, E. A., Möbius, E., Scholer, M., Thomsen, M. F., and Walker, S. N.: Cluster at the Bow Shock: Introduction, Space Sci. Rev., 118, 155–160, https://doi.org/10.1007/s11214-005-3826-1, 2005.

Burch, J. L.and Moore, T. E., Torbert, R. B., and Giles, B. L.: Magnetospheric Multiscale Overview and Science Objectives, Space Sci. Rev., 199, 5–21, https://doi.org/10.1007/s11214-015-0164-9, 2016.

Dmitriev, A. V. and Suvorova, A. V.: Large-scale jets in the magnetosheath and plasma penetration across the magnetopause: THEMIS observations, J. Geophys. Res.-Space, 120, 4423–4437, https://doi.org/https://doi.org/10.1002/2014JA020953, 2015.

Dmitriev, A. V. and Suvorova, A. V.: Atmospheric Effects of Magnetosheath Jets, Atmosphere, 14, https://doi.org/10.3390/atmos14010045, 2023.

Eastwood, J. P., Lucek, E. A., Mazelle, C., Meziane, K., Narita, Y., Pickett, J., and Treumann, R. A.: The Foreshock, Space Sci. Rev., 118, 41–94, https://doi.org/10.1007/s11214-005-3824-3, 2005.

Escoubet, C., Fehringer, M., and Goldstein, M.: The Cluster mission, Ann. Geophys., 19, 1197–1200, https://doi.org/10.5194/angeo-19-1197-2001, 2001.

Grimes, E. W., Lewis, J. W., Angelopoulos, V., McTiernan, J. M., Hatzigeorgiu, N., Drozdov, A., and Russell, C.: Pyspedas, a Python Implementation of SPEDAS, in: AGU Fall Meeting Abstracts, vol. 2018, pp. IN11B–0629, 2018.

Gunell, H., Stenberg Wieser, G., Mella, M., Maggiolo, R., Nilsson, H., Darrouzet, F., Hamrin, M., Karlsson, T., Brenning, N., De Keyser, J., André, M., and Dandouras, I.: Waves in high-speed plasmoids in the magnetosheath and at the magnetopause, Ann. Geophys., 32, 991–1009, https://doi.org/10.5194/angeo-32-991-2014, 2014.

Han, D.-S., Hietala, H., Chen, X.-C., Nishimura, Y., Lyons, L. R., Liu, J.-J., Hu, H.-Q., and Yang, H.-G.: Observational properties of dayside throat aurora and implications on the possible generation mechanisms, J. Geophys. Res.-Space, 122, 1853–1870, https://doi.org/https://doi.org/10.1002/2016JA023394, 2017.

Hietala, H., Laitinen, T. V., Andréeová, K., Vainio, R., Vaivads, A., Palmroth, M., Pulkkinen, T. I., Koskinen, H. E. J., Lucek, E. A., and Rème, H.: Supermagnetosonic Jets behind a Collisionless Quasiparallel Shock, Phys. Rev. Lett., 103, 245 001, https://doi.org/10.1103/PhysRevLett.103.245001, 2009.

https://doi.org/10.5194/angeo-2023-31
Preprint. Discussion started: 4 October 2023

Hietala, H., Partamies, N., Laitinen, T. V., Clausen, L. B. N., Facskó, G., Vaivads, A., Koskinen, H. E. J., Dandouras, I., Rème, H., and Lucek, E. A.: Supermagnetosonic subsolar magnetosheath jets and their effects: from the solar wind to the ionospheric convection, Ann. Geophys., 30, 33–48, https://doi.org/10.5194/angeo-30-33-2012, 2012.

Hietala, H., Phan, T. D., Angelopoulos, V., Oieroset, M., Archer, M. O., Karlsson, T., and Plaschke, F.: In Situ Observations of a Magnetosheath High-Speed Jet Triggering Magnetopause Reconnection, Geophys. Res. Lett., 45, 1732–1740, https://doi.org/https://doi.org/10.1002/2017GL076525, 2018.

Karlsson, T., Brenning, N., Nilsson, H., Trotignon, J.-G., Vallières, X., and Facsko, G.: Localized density enhancements in the magnetosheath: Three-dimensional morphology and possible importance for impulsive penetration, J. Geophys. Res.-Space, 117, https://doi.org/https://doi.org/10.1029/2011JA017059, 2012.

Karlsson, T., Plaschke, F., Hietala, H., Archer, M., Blanco-Cano, X., Kajdič, P., Lindqvist, P.-A., Marklund, G., and Gershman, D. J.: Investigating the anatomy of magnetosheath jets – MMS observations, Ann. Geophys., 36, 655–677, https://doi.org/10.5194/angeo-36-655-2018, 2018.

King, J. H. and Papitashvili, N. E.: Solar wind spatial scales in and comparisons of hourly Wind and ACE plasma and magnetic field data, J. Geophys. Res.-Space, 110, https://doi.org/https://doi.org/10.1029/2004JA010649, 2005.

Koller, F., Plaschke, F., Temmer, M., Preisser, L., Roberts, O. W., and Vörös, Z.: Magnetosheath Jet Formation Influenced by Parameters in Solar Wind Structures, J. Geophys. Res.-Space, 128, e2023JA031 339, https://doi.org/https://doi.org/10.1029/2023JA031339, 2023.

LaMoury, A. T., Hietala, H., Plaschke, F., Vuorinen, L., and Eastwood, J. P.: Solar Wind Control of Magnetosheath Jet Formation and Propagation to the Magnetopause, J. Geophys. Res.-Space, 126, e2021JA029 592, https://doi.org/https://doi.org/10.1029/2021JA029592, e2021JA029592 2021JA029592, 2021.

McFadden, J., Carlson, C., Larson, D., Ludlam, M., Abiad, R., Elliott, B., Turin, P., Marckwordt, M., and Angelopoulos, V.: The THEMIS ESA Plasma Instrument and In-flight Calibration, Space Sci. Rev., 141, 277–302, https://doi.org/10.1007/s11214-008-9440-2, 2008.

Němeček, Z., Šafránková, J., Přech, L., Sibeck, D. G., Kokubun, S., and Mukai, T.: Transient flux enhancements in the magnetosheath, Geophys. Res. Lett., 25, 1273–1276, https://doi.org/https://doi.org/10.1029/98GL50873, 1998.

Nykyri, K., Bengtson, M., Angelopoulos, V., Nishimura, Y., and Wing, S.: Can Enhanced Flux Loading by High-Speed Jets Lead to a Substorm? Multipoint Detection of the Christmas Day Substorm Onset at 08:17 UT, 2015, J. Geophys. Res.-Space, 124, 4314–4340, https://doi.org/https://doi.org/10.1029/2018JA026357, 2019.

OMNI: Solar wind data from NASA's OMNI high resolution data set, available at: https://omniweb.gsfc.nasa.gov/ow_min.html, last access: 05 September 2023, 2023.

Palmroth, M., Raptis, S., Suni, J., Karlsson, T., Turc, L., Johlander, A., Ganse, U., Pfau-Kempf, Y., Blanco-Cano, X., Akhavan-Tafti, M., Battarbee, M., Dubart, M., Grandin, M., Tarvus, V., and Osmane, A.: Magnetosheath jet evolution as a function of lifetime: global hybrid-Vlasov simulations compared to MMS observations, Ann. Geophys., 39, 289–308, https://doi.org/10.5194/angeo-39-289-2021, 2021.

Plaschke, F. and Hietala, H.: Plasma flow patterns in and around magnetosheath jets, Ann. Geophys., 36, 695–703, https://doi.org/10.5194/angeo-36-695-2018, 2018.

Plaschke, F., Hietala, H., and Angelopoulos, V.: Anti-sunward high-speed jets in the subsolar magnetosheath, Ann. Geophys., 31, 1877–1889, https://doi.org/10.5194/angeo-31-1877-2013, 2013.

Plaschke, F., Hietala, H., Angelopoulos, V., and Nakamura, R.: Geoeffective jets impacting the magnetopause are very common, J. Geophys. Res.-Space, 121, 3240–3253, https://doi.org/https://doi.org/10.1002/2016JA022534, 2016.

https://doi.org/10.5194/angeo-2023-31
Preprint. Discussion started: 4 October 2023

Plaschke, F., Karlsson, T., Hietala, H., Archer, M., Vörös, Z., Nakamura, R., Magnes, W., Baumjohann, W., Torbert, R. B., Russell, C. T., and Giles, B. L.: Magnetosheath High-Speed Jets: Internal Structure and Interaction With Ambient Plasma, J. Geophys. Res.-Space, 122, 10,157–10,175, https://doi.org/https://doi.org/10.1002/2017JA024471, 2017.

Plaschke, F., Hietala, H., Archer, M. O., Blanco-Cano, X., Kajdič, P., Karlsson, T., Lee, S. H., Omidi, N., Palmroth, M., Roytershteyn, V., Schmid, D., Sergeev, V., and Sibeck, D.: Jets Downstream of Collisionless Shocks, Space Sci. Rev., 214, https://doi.org/10.1007/s11214-018-0516-3, 2018.

Plaschke, F., Hietala, H., and Vörös, Z.: Scale Sizes of Magnetosheath Jets, J. Geophys. Res.-Space, 125, e2020JA027 962, https://doi.org/https://doi.org/10.1029/2020JA027962, 2020a.

Plaschke, F., Jernej, M., Hietala, H., and Vuorinen, L.: On the alignment of velocity and magnetic fields within magnetosheath jets, Ann. Geophys., 38, 287–296, https://doi.org/10.5194/angeo-38-287-2020, 2020b.

Raptis, S., Karlsson, T., Plaschke, F., Kullen, A., and Lindqvist, P.-A.: Classifying Magnetosheath Jets Using MMS: Statistical Properties, J. Geophys. Res.-Space, 125, e2019JA027 754, https://doi.org/https://doi.org/10.1029/2019JA027754, e2019JA027754 10.1029/2019JA027754, 2020.

Raptis, S., Karlsson, T., Vaivads, A., Pollock, C., Plaschke, F., Johlander, A., Trollvik, H., and Lindqvist, P.-A.: Downstream high-speed plasma jet generation as a direct consequence of shock reformation, Nat. Commun., 13, 598, https://doi.org/10.1038/s41467-022-28110-4, 2022.

Savin, S., Amata, E., Zelenyi, L., Lutsenko, V., Safrankova, J., Nemecek, Z., Borodkova, N., Buechner, J., Daly, P. W., Kronberg, E. A., Blecki, J., Budaev, V., Kozak, L., Skalsky, A., and Lezhen, L.: Super fast plasma streams as drivers of transient and anomalous magnetospheric dynamics, Ann. Geophys., 30, 1–7, https://doi.org/10.5194/angeo-30-1-2012, 2012.

Schwartz, S. J. and Burgess, D.: Quasi-parallel shocks: A patchwork of three-dimensional structures, Geophys. Res. Lett., 18, 373–376, https://doi.org/https://doi.org/10.1029/91GL00138, 1991.

Shue, J.-H., Chao, J.-K., Song, P., McFadden, J. P., Suvorova, A., Angelopoulos, V., Glassmeier, K. H., and Plaschke, F.: Anomalous magnetosheath flows and distorted subsolar magnetopause for radial interplanetary magnetic fields, Geophys. Res. Lett., 36, https://doi.org/https://doi.org/10.1029/2009GL039842, 2009.

Spreiter, J. R., Summers, A. L., and Alksne, A. Y.: Hydromagnetic flow around the magnetosphere, Planet. Space Sci., 14, 223–253, https://doi.org/https://doi.org/10.1016/0032-0633(66)90124-3, 1966.

Suni, J., Palmroth, M., Turc, L., Battarbee, M., Johlander, A., Tarvus, V., Alho, M., Bussov, M., Dubart, M., Ganse, U., Grandin, M., Horaites, K., Manglayev, T., Papadakis, K., Pfau-Kempf, Y., and Zhou, H.: Connection Between Foreshock Structures and the Generation of Magnetosheath Jets: Vlasiator Results, Geophys. Res. Lett., 48, e2021GL095 655, https://doi.org/https://doi.org/10.1029/2021GL095655, 2021.

THEMIS: THEMIS mission including level 2 FGM and ESA data, available at: http://themis.ssl.berkeley.edu/data/themis, last access: 05 September 2023, 2023.

Vuorinen, L., Hietala, H., and Plaschke, F.: Jets in the magnetosheath: IMF control of where they occur, Ann. Geophys., 37, 689–697, https://doi.org/10.5194/angeo-37-689-2019, 2019.